Abstract 1462

Three-Dimensional Documentation of the Transition from Sand Ripples to Megaripples

James R. Zimbelman[1], Stephen P. Scheidt[2], Mariah M. Baker[1], Edward Williams[3]

[1]CEPS/NASM, MRC 315, Smithsonian Institution, Washington, D.C. 20013-7012, zimbelmanj@si.edu; [2]Planetary Science Institute, Odenton, MD 21112; [3]Department of Geology, U. of Maryland, College Park, MD 20742

Introduction: The transition from sand ripples to megaripples encodes information about the physics of how both sand-sized (moved via saltation) and coarse-grained (moved via impact creep) particles interact under Martian conditions. Previous studies have focused on the aeolian mobility of sand on Mars; here we examine how mobile sand interacts with larger particles moved by creep. HiRISE images of small dunes (lacking well developed slip faces) on Mars reveal a transition of aeolian bedform scale with increasing distance from the dune [1]. Here we document the particles in a similar transition on Earth.

Background: High Resolution Imaging Science Experiment (HiRISE [2]) images have documented that sand is moving at many locations around Mars under current conditions [3-5]. Unlike these many active sand deposits, enigmatic "Transverse Aeolian Ridges" (TARs; the non-genetic term for linear to curvilinear aeolian bedforms resulting from either dune- or ripple-forming processes [6]) showed no evidence of movement anywhere across Mars [7-9]. Recently bright TARs were documented to have moved in HiRISE images taken many Earth years apart at three widely separated locations [10]. Great Sand Dunes National Park and Preserve (GSDNPP) in Colorado [11] has a bimodal particle size distribution along with a seasonal bimodal wind regime, providing the setting to examine the transition from sand ripples (<1 cm in height) to megaripples (typically ~25 cm in height).

Results: A Smithsonian Scholarly Studies Award for FY19 funded trips to GSDNPP during May and September of 2019 to collect thousands of digital photographs of ripple-megaripple transitions that were later processed using Multiview Stereo Photogrammetry (MVSP) to produce detailed Digital Terrain Models (DTMs; Fig. 1). The digital images were obtained using a Nikon camera motor-driven along a track above the study area. The track was manually advanced several cm after each photo traverse. Photos were obtained using both a 35 mm lens (Fig. 2) and a 85 mm Macro lens. The DTMs resolve both sand ripple and megaripple bedforms (Fig. 3) and coarse particles (1-2-mm diameter) on the bedforms (Fig. 4), providing a detailed record of the surface distribution of coarse grains across the bedforms at multiple scales.

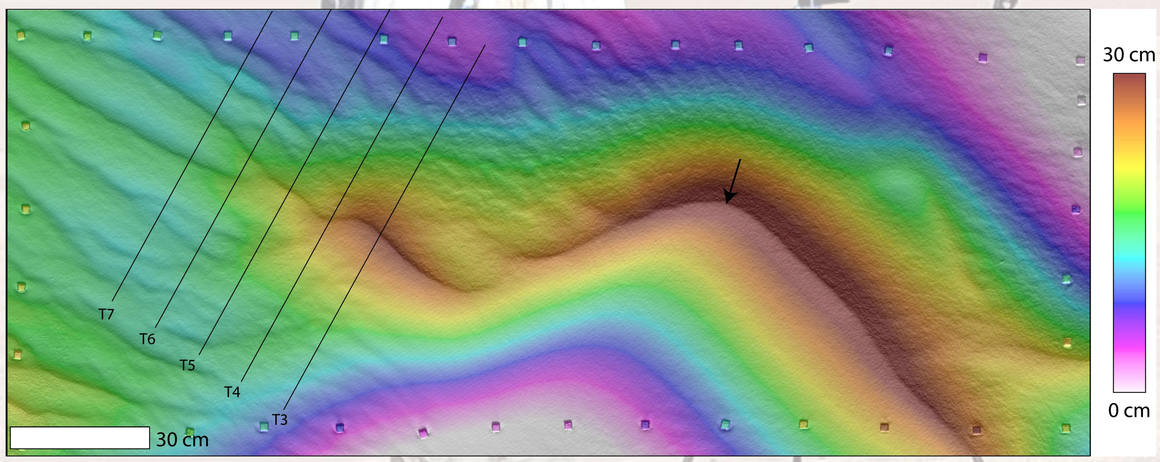

Figure 1. Colorized DTM of study area at GSDNPP (5-30-19) Site slopes 11° to S30E, so height here increases relative to 0 at the upper left. Orthophotomosaic of same area is in Fig 2. Lines indicate transects across the transition from sand ripples to megaripples (T3 to T7; see Fig. 3). Arrow indicates location of Fig. 4. Data generated by MVSP using images taken at a 35 mm focal length.

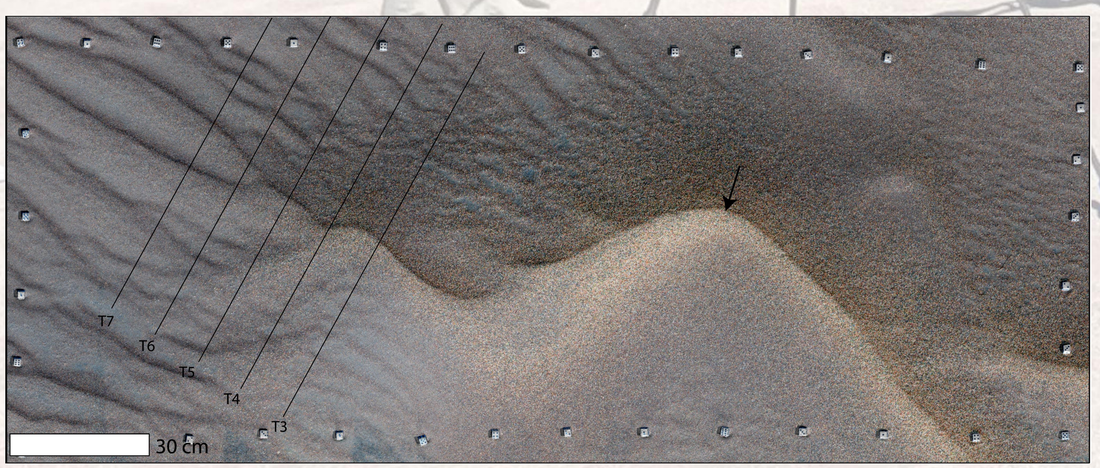

Figure 2. Orthophotomosaic of study area in Fig. 1 (above), outlined by dice 1.6 cm wide. Colors have been stretched by normalizing the color histograms, highlighting the color difference between feldspar-rich granules on the megaripple crest and the more mafic sand.

Trenching of bedforms revealed that often both sand ripples and megaripples are coated by a layer of coarse particles that become increasingly more closely packed approaching the crest of the bedform. Coarse grains are stacked several particles deep at the crests of megaripples, a condition common on many megaripples [e.g. 12, 13]. Under strong (>8 m/s at 50 cm above the surface) wind conditions, we observed coarse particles to either roll or move several millimeters when impacted by saltating sand. We did not observe that sand ripples are a necessary prerequisite for the initiation or growth of megaripples, but the two bedform scales do interact because the rate of bedform movement is proportional to bedform height [14], so that sand ripples overtake the larger megaripples. The spatial density of coarse particles does appear to influence the growth of ripples, when the coarse particles become so closely packed that the underlying sand is no longer exposed to saltating sand. We intend to explore this relationship quantitatively as more DTM data becomes available.

Application to Mars: There is abundant evidence from rover images that ripples of multiple sizes and wavelengths are common on Mars [15-18]. Curiosity images include many examples of interactions between sand ripples and megaripples (Fig. 2). TARs observed in orbital images [6-9, 19] are much larger than most ripples or megaripples seen by rovers, with the one exception of the large bedform crossed by Curiosity at Dingo Gap [20, 21]. In order to assess how effectively ripple-megaripple transitions can be detected from orbit, a project during the summer of 2019 examined three HiRISE images covering portions of Nirgal Vallis, a sapping channel whose floor is nearly completely covered by TARs [22]. We documented ripple-megaripple transitions displaying continuous crests at 1/5th of all TAR crest terminations, out of 1570 terminations examined in the three images. Additionally, 1/3 of the TAR crest terminations had 'probable' transitions, so <1/2 of TAR crest terminations lacked evidence of a transition.

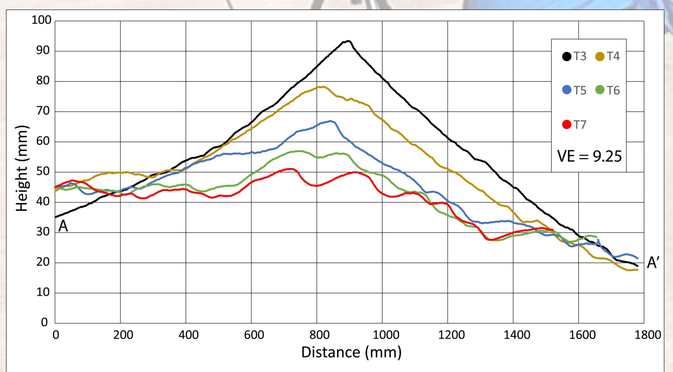

Figure 3. Topographic profiles across the sand-ripple-to-megaripple transition (profiles T3 to T7; see Figs. 1 and 2), measured orthogonal to the mean crest orientation. Each profile has a vertical exaggeration of 9.25X.

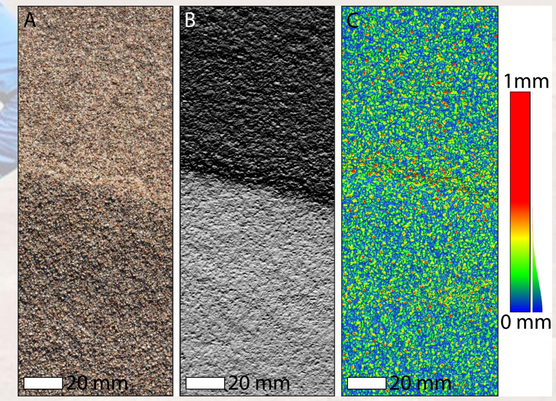

Figure 4. Detail extracted from images taken with an 85 mm Macro lens. Area shown is 80 x 200 mm across the crest of a megaripple (arrow in Figs. 1 and 2). A. Orthophotomosaic generated by MVSP, gridded at 0.05 mm. B. Hillshade of DTM (sun angle is 25° above horizontal at 180° azimuth) gridded at 0.2 mm. C. Map of surface roughness (individual particles), gridded at 0.05 mm. Each pixel is calculated as the elevation difference from the average elevation of a sliding local 2 mm kernel window.

Figure 5. Ripple-megaripple interactions in a Curiosity Mastcam mosaic, Enchanted Island, sol 1752. NASA/JPL-Caltech/MSSS. [After Fig. 1d of 17].

References: [1] Zimbelman, J. R. (2019) Icarus 333, 127-129, doi: 10.1016/j.icarus.2019.05.017. [2] McEwen, A.S., et al. (2007) JGR-Planets 112, E05S02, doi: 10.1029/2005JE002605. [3] Silvestro, S., et al., (2010) GRL 37, L20203, doi: 10.1016/ j.icarus.2019.05.017. [4] Bridges, N., et al. (2012) Geology 40, 31-34, doi: 10.1130/G32373.1. [5] Banks, M. E., et al. (2018) JGR-Planets 123, 3205-3219, doi:10.1029/2018JE005747. [6] Bourke, M.C., et al. (2003) LPS XXXIV, Abs# 2090. [7] Wilson, S. A., J. R. Zimbelman (2004) JGR-Planets 109, E10003, 10.1029/2004JE002247. [8] Balme et al., 2008. [9] Berman et al., 2011, 2018. [10] Silvestro, S., et al. (2019) LPS L, Abs# 1800. [11] Madole, R. F., et al. (2008) Geomorph. 99, 99-119. [12] Sharp, R. P. (1963) J. Geol. 71, 617-636. [13] de Silva, S. L., et al. (2013) GSAB 125 (11/12), 1912-1929, doi: 10.1130/B30916.1. [14] Bagnold, R. A. (1941) The physics of blown sand and desert dunes. Chapman and Hall, London. [15] Sullivan, R.S., et al. (2005) Nature 436, doi: 10.1038/nature03641. [16] Sullivan, R. S., et al. (2008) JGR-Planets 113, E06S07, doi:10.1029/2008JE003101. [17] Lapotre, M. G. A., et al. (2018) GRL 45, 10,229-10,239, doi: 10.1029/2018GL079029. [18] Baker, M. M., et al. (2018) GRL 45, 8853-8863, doi: 10.1029/2018GL079040. [19.] Zimbelman, J. R. (2010) Geomorphology 121, 22-29, doi:10.10.1016/j.geomorph.2009.05.012. [20] Day, M., Kokurek, G. (2016) Icarus 280, 37-71, doi: 10.1016/j.Icarus.2015.09.042. [21] Zimbelman, J. R., Foroutan, M. (2017) Fifth International Planetary Dunes Workshop, LPI Contribution 1961, Abs. #3037. [22] Reiss, D., et al. (2004) GRL 109, E06007, doi: 10.1029/2004JE002251